Effect of Substituents on the Formation of Vinylideneruthenium(II) Complexes. X-ray Structures of $RuCl_2\{=C=C(Z)Ph\}(dcpmp)$ (Z = H, $SiMe_3$; dcpmp = $C_5H_3N(CH_2PCy_2)_2$)

Hiroyuki Katayama,* Chikaya Wada, Ken Taniguchi, and Fumiyuki Ozawa*

Department of Applied Chemistry, Graduate School of Engineering, Osaka City University, Sumiyoshi-ku, Osaka 558-8585, Japan

Received March 28, 2002

Kinetic studies have been carried out for the formation of vinylideneruthenium(II) complexes $RuCl_2\{=C=C(Z)R\}(dcpmp)$ [Z = H, R = *p*-$MeOC_6H_4$ (**2a**), *p*-MeC_6H_4 (**2b**), Ph (**2c**), *p*-BrC_6H_4 (**2d**), *t*-Bu (**2e**), ferrocenyl (**2f**); Z = $SiMe_3$, R = Ph (**5a**), $SiMe_3$ (**5b**); dcpmp = 2,6-bis{(dicyclohexylphosphino)methyl}pyridine] from $RuCl_2(NCMe)(dcpmp)$ (**1**) and alkynes (RC≡CZ). The reactions with terminal alkynes proceed via preliminary dissociation of the MeCN ligand from **1**, giving vinylidene complexes **2a**−**2f** in quantitative yields. More electron-rich and less sterically demanding alkynes tend to provide higher reaction rates. On the other hand, the reactions with silylalkynes afford equilibrium mixtures of **1** and *β*-silylvinylidene complexes **5**. The X-ray structures of **2c** and **5a** are reported.

Introduction

It has become apparent that ruthenium-catalyzed organic transformation of alkynes often involves vinylidene intermediates.[1] Representative reactions include homo- and co-dimerization of terminal alkynes,[2] cross-coupling reactions of alkynes with alkenes,[3] cycloaromatization of conjugated enediynes,[4] cyclocarbonylation of diynes,[5] and addition of oxygen-nucleophiles to alkynes.[6−8] It has been also documented that vinylidene complexes of the type $RuCl_2(=C=CHR)L_2$ (L = PPr^i_3, PCy_3) serve as good catalyst precursors for ring-opening metathesis polymerization of cycloalkenes and ring-closing metathesis reactions of α,*ω*-dienes.[9] Vinylidene complexes responsible for these catalyses are generally afforded by tautomerization of alkyne ligands via a 1,2-hydrogen shift (eq 1). A similar tautomeriza-

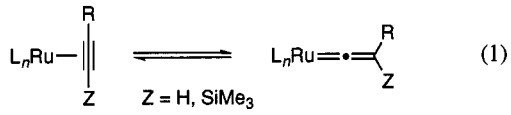

(1)

tion process has been observed for silylalkynes, which undergo 1,2-migration of the silyl group to afford *β*-silylvinylidene complexes.[10,11] Consequently, catalytic reactions involving vinylidene intermediates must be significantly affected by kinetic and thermodynamic features of the interconversion given in eq 1, while the

* To whom correspondence should be addressed. Fax: +81 666052978. E-mail: katayama@a-chem.eng.osaka-cu.ac.jp; ozawa@a-chem.eng.osaka-cu.ac.jp.

(1) For a review, see: Bruneau, C.; Dixneuf, P. H. *Acc. Chem. Res.* **1999**, *32*, 311−323.

(2) (a) Baratta, W.; Del Zotto, A.; Herdtweck, E.; Vuano, S.; Rigo, P. *J. Organomet. Chem.* **2001**, *617*−*618*, 511−519. (b) Tenorio, M. A. J.; Tenorio, M. J.; Puerta, M. C.; Valerga, P. *Organometallics* **2000**, *19*, 1333−1342. (c) Bassetti, M.; Marini, S.; Tortorella, F.; Cadierno, V.; Díez, J.; Gamasa, M. P.; Gimeno, J. *J. Organomet. Chem.* **2000**, *593*−*594*, 292−298. (d) Baratta, W.; Herrmann, W. A.; Rigo, P.; Schwarz, J. *J. Organomet. Chem.* **2000**, *593*−*594*, 489−493. (e) Nishibayashi, Y.; Yamanashi, M.; Wakiji, I.; Hidai, M. *Angew. Chem., Int. Ed.* **2000**, *39*, 2909−2911. (f) Yi, C. S.; Liu, N. *Organometallics* **1998**, *17*, 3158−3160. (g) Qü, J.-P.; Masui, D.; Ishii, Y.; Hidai, M. *Chem. Lett.* **1998**, 1003−1004. (h) Yi, C. S.; Liu, N.; Rheingold, A. L.; Liable-Sands, L. M. *Organometallics* **1997**, *16*, 3910−3913, and references therein.

(3) Murakami, M.; Ubukata, M.; Ito, Y. *Tetrahedron Lett.* **1998**, *39*, 7361−7364.

(4) Wang, Y.; Finn, M. G. *J. Am. Chem. Soc.* **1995**, *117*, 8045−8046.

(5) Onitsuka, K.; Katayama, H.; Sonogashira, K.; Ozawa, F. *J. Chem. Soc., Chem. Commun.* **1995**, 2267−2268.

(6) (a) Trost, B. M.; Vidal, B.; Thommen, M. *Chem. Eur. J.* **1999**, *5*, 1055−1069. (b) Trost, B. M.; Kulawiec, R. J. *J. Am. Chem. Soc.* **1992**, *114*, 5579−5584. (c) Trost, B. M.; Dyker, G.; Kulawiec, R. *J. Am. Chem. Soc.* **1990**, *112*, 7809−7811.

(7) (a) Doucet, H.; Derrien, N.; Kabouche, Z.; Bruneau, C.; Dixneuf, P. H. *J. Organomet. Chem.* **1997**, *551*, 151−157. (b) Gemel, C.; Trimmel, G.; Slugovc, C.; Kremel, S.; Mereiter, K.; Schmid, R.; Kirchner, K. *Organometallics* **1996**, *15*, 3998−4004. (c) Doucet, H.; Martin-Vaca, B.; Bruneau, C.; Dixneuf, P. H. *J. Org. Chem.* **1995**, *60*, 10901−10912. (d) Höfer, J.; Doucet, H.; Bruneau, C.; Dixneuf, P. H. *Tetrahedron Lett.* **1991**, *32*, 7409−7410. (e) Mahé, R.; Sasaki, Y.; Bruneau, C.; Dixneuf, P. H. *J. Org. Chem.* **1989**, *54*, 1518−1523. (f) Mahé, R.; Dixneuf, P. H.; Lécolier, S. *Tetrahedron Lett.* **1986**, *27*, 6333−6336.

(8) (a) Suzuki, T.; Tokunaga, M.; Wakatsuki, Y. *Org. Lett.* **2001**, *3*, 735−737. (b) Tokunaga, M.; Wakatsuki, Y. *Angew. Chem., Int. Ed.* **1998**, *37*, 2867−286.

(9) (a) Katayama, H.; Urushima, H.; Ozawa, F. *J. Organomet. Chem.* **2000**, *606*, 16−25. (b) Katayama, H.; Urushima, H.; Ozawa, F. *Chem. Lett.* **1999**, 369−370. (c) Katayama, H.; Ozawa, F. *Chem. Lett.* **1998**, 67−68.

(10) For ruthenium, see: (a) Katayama, H.; Ozawa, F. *Organometallics* **1998**, *17*, 5190−5196. (b) Huang, D.; Streib, W. E.; Bollinger, J. C.; Caulton, K. G.; Winter, R. F.; Scheiring, T. *J. Am. Chem. Soc.* **1999**, *121*, 8087−8097.

(11) For other transition metals, see: (a) Foerstner, J.; Kakoschke, A.; Goddard, R.; Rust, J.; Wartchow, R.; Butenschön, H. *J. Organomet. Chem.* **2001**, *617*−*618*, 412−422. (b) Gauss, C.; Veghini, D.; Berke, H. *Chem. Ber./Recl.* **1997**, *130*, 183−194. (c) Connelly, N. G.; Geiger, W. E.; Lagunas, M. C.; Metz, B.; Rieger, A. L.; Rieger, P. H.; Shaw, M. *J. Am. Chem. Soc.* **1995**, *117*, 12202−12208. (d) Naka, A.; Okazaki, S.; Hayasi, M.; Ishikawa, M. *J. Organomet. Chem.* **1995**, *499*, 35−41. (e) Werner, H.; Baum, M.; Schneider, D.; Windmüller, B. *Organometallics* **1994**, *13*, 1089−1097. (f) Sakurai, H.; Fujii, T.; Sakamoto, K. *Chem. Lett.* **1992**, 339−342.

10.1021/om020238r CCC: $22.00
Publication on Web 06/25/2002

detailed information on this process, particularly on the effects of substituent R, has so far been extremely limited.[12]

Previously, we examined interconversion between silylalkyne and β-silylvinylidene complexes of rhodium by kinetic experiments. This study revealed that thermodynamic stability of vinylidene complexes increases as the R substituent becomes more electron-donating.[13] The present paper reports a related study on ruthenium complexes. Using 2,6-bis{(dicyclohexylphosphino)methyl}-pyridine (dcpmp) as a supporting ligand, we could observe kinetic and thermodynamic data for alkyne−vinylidene interconversion on ruthenium.

Results

Reactions of $RuCl_2$(NCMe)(dcpmp) (1) with Terminal Alkynes. A simple and clean reaction system is needed to perform kinetic investigations. After several attempts, we found $RuCl_2$(NCMe)(dcpmp) (**1**) as the starting material of choice in this respect. This complex cleanly reacts with a variety of terminal alkynes at convenient reaction temperatures for kinetic experiments, giving the corresponding vinylidene complexes (**2a**−**2f**) in quantitative yields (eq 2).

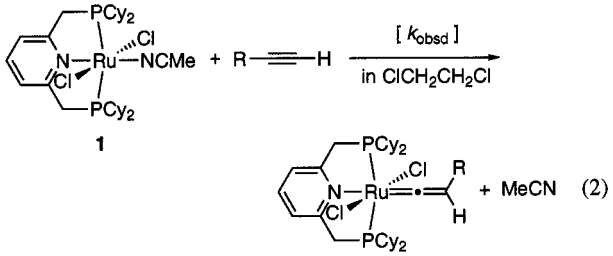

2a: R = *p*-$MeOC_6H_4$
2b: R = *p*-MeC_6H_4
2c: R = Ph
2d: R = *p*-BrC_6H_4
2e: R = *t*-Bu
2f: R = Fc

Complex **1** was prepared in 65% isolated yield by treating $[RuCl_2(p\text{-cymene})]_2$ with dcpmp (1 equiv/Ru) in toluene in the presence of excess MeCN (10 equiv/Ru) at 80 °C for 22 h and identified by NMR spectroscopy and elemental analysis. The $^{31}P\{^1H\}$ NMR spectrum exhibited a sharp singlet at δ 44.6. The ^1H NMR spectrum was consistent with a C_{2v} symmetrical structure involving meridional coordination of the PNP ligand. Thus the PCH_2 protons were observed as a virtual triplet at δ 3.72 (J_{app} = 4.2 Hz), showing a trans arrangement of the two phosphorus atoms. The signals arising from the pyridine ring appeared at δ 7.23 and 7.04 in an apparent AX_2 pattern ($^3J_{HH}$ = 7.5 Hz). The presence of the MeCN ligand was clearly indicated by the occurrence of a methyl proton signal at δ 2.35 in the ^1H NMR spectrum and of a ν(C≡N) absorption at 2265 cm^{-1} in the IR spectrum.

The reaction of **1** with PhC≡CH (>10 equiv) in $ClCH_2CH_2Cl$ was followed by $^{31}P\{^1H\}$ NMR spectroscopy. The formation of vinylidene complex **2c** obeyed good pseudo-first-order kinetics over 85% conversion of **1**. Table 1 lists the rate constants measured at various reaction conditions. No ruthenium species other than **1** and **2c** were detected in all kinetic runs.

Table 1. Pseudo-First-Order Rate Constants for the Reaction of 1 with PhC≡CH in $ClCH_2CH_2Cl$ at 50 °C[a]

run	[PhC≡CH] (mM)	[MeCN] (mM)[b]	$10^4 k_{obsd}$ (s^{-1})
1	160	74	2.67(3)
2	210	74	3.5(1)
3	300	74	4.75(4)
4	320	74	5.04(5)
5	380	74	5.67(6)
6	150	0	9.6(3)
7	150	19	8.86(9)
8	150	40	4.71(6)
9	150	60	3.8(1)
10	150	79	2.74(9)
11	150	127	1.78(4)
12[c]	150 (PhC≡CD)	40	2.79(4)

[a] Initial concentration: $[\mathbf{1}]_0$ = 15 mM. [b] The concentration of free MeCN added to the system. [c] The reaction was performed with PhC≡CD instead of PhC≡CH.

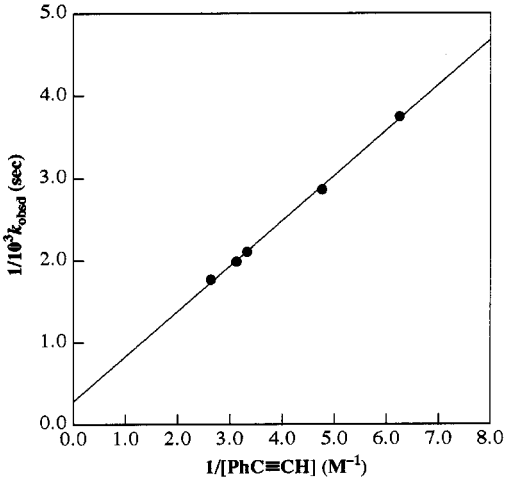

Figure 1. Effect of PhC≡CH concentration on the reaction rate of **1** with PhC≡CH in $ClCH_2CH_2Cl$ at 50 °C in the presence of added MeCN. Initial concentration: $[\mathbf{1}]_0$ = 15 mM, $[MeCN]_0$ = 74 mM.

The reaction rate increased with increasing concentration of PhC≡CH (runs 1−5). A good linear correlation (r = 1.000) was observed between $1/k_{obsd}$ and 1/[PhC≡CH] values (Figure 1). On the other hand, the reaction was effectively retarded by addition of free MeCN to the system (runs 6−11); the $1/k_{obsd}$ values were linearly correlated with the concentration of added MeCN (Figure 2, r = 0.998). Furthermore, a moderate kinetic isotope effect (k_H/k_D = 1.69(5)) was noted in the reaction with deuterated phenylacetylene (run 12).

These kinetic observations clearly suggest the mechanism depicted in Scheme 1. The coordinatively saturated complex **1** undergoes reversible dissociation of the MeCN ligand. The five-coordinate intermediate **3** thus generated subsequently reacts with PhC≡CH to give the vinylidene complex **2c**, very probably via a phenylacetylene-coordinated intermediate **4c**. Steady-state approximation for the concentration of **3** leads to the kinetic expressions given in eqs 3 and 4, in which the rate constants k_1 and k_{-1} correspond to the forward and

(12) (a) Ajioka, Y.; Matsushima, Y.; Onitsuka, K.; Yamazaki, H.; Takahashi, S. *J. Organomet. Chem.* **2001**, *617*−*618*, 601−615. (b) de los Ríos, I.; Tenorio, M. J.; Puerta, M. C.; Valerga, P. *J. Am. Chem. Soc.* **1997**, *119*, 6529−6538.

(13) Katayama, H.; Onitsuka, K.; Ozawa, F. *Organometallics* **1996**, *15*, 4642−4645.

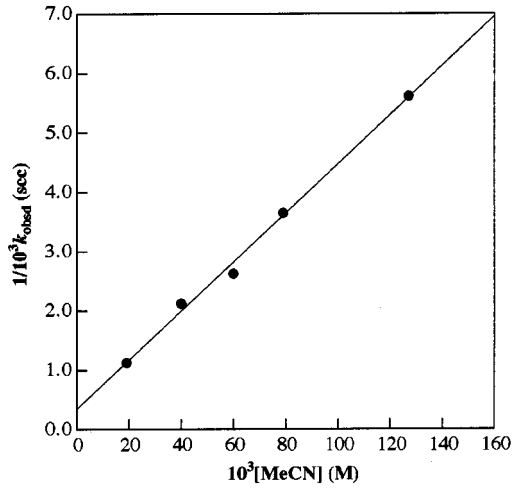

Figure 2. Effect of added MeCN on the reaction rate of **1** with PhC≡CH in $ClCH_2CH_2Cl$ at 50 °C. Initial concentration: $[\mathbf{1}]_0 = 15$ mM, $[PhC{\equiv}CH]_0 = 150$ mM.

Scheme 1

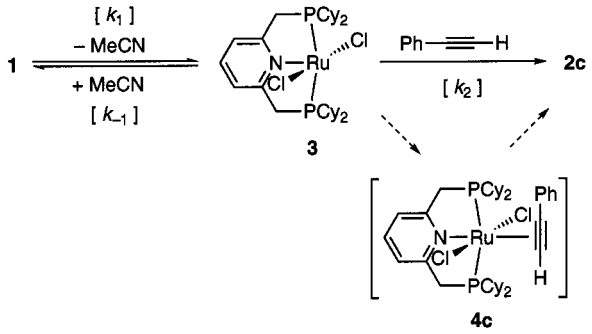

backward reactions between **1** and **3**, respectively, and k_2 to the overall process from **3** to **2c**.

$$-\frac{d[\mathbf{1}]}{dt} = \frac{d[\mathbf{2c}]}{dt} = k_{obsd}[\mathbf{1}] = \frac{k_1 k_2[PhC{\equiv}CH]}{k_{-1}[MeCN] + k_2[PhC{\equiv}CH]}[\mathbf{1}] \quad (3)$$

$$\frac{1}{k_{obsd}} = \frac{k_{-1}[MeCN]}{k_1 k_2[PhC{\equiv}CH]} + \frac{1}{k_1} \quad (4)$$

On the basis of the slope and intercept of the plot in Figure 1, the values of k_1 and k_{-1}/k_2 are estimated as 3.0×10^{-3} s^{-1} and 22, respectively, which are in good agreement with the values derived from the plot in Figure 2 ($k_1 = 2.9 \times 10^{-3}$ s^{-1}, $k_{-1}/k_2 = 18$). The k_1 value corresponds to $\Delta G^{\ddagger}_{323} = 22.7$ kcal mol^{-1}. On the other hand, the k_{-1}/k_2 ratio indicates that the re-coordination of MeCN to **3** to give **1** is easier by 1.9 kcal mol^{-1} than the conversion of **3** into **2c**. These kinetic features, in conjunction with the observation of a clear deuterium kinetic isotope effect, clearly suggest a significant contribution of the rate of phenylacetylene–phenylvinylidene tautomerization toward the k_{obsd} value, even though the dissociation of MeCN from **1** constitutes the slowest step in the overall process.

Table 2 compares the reactivity of seven kinds of terminal alkynes under the same reaction conditions. There is a tendency that the more electron-donating substituent at the para position of phenylacetylene leads to the higher reaction rate (runs 1–5). *tert*-Butylacetylene is moderately reactive probably due to its bulkiness (run 6), while ferrocenylacetylene (FcC≡CH) exhibits the highest reactivity (run 7).

Table 2. Pseudo-First-Order Rate Constants for the Reactions of 1 with Various Terminal Alkynes[a]

run	alkyne	product	$10^4 k_{obsd}$ (s^{-1})
1	*p*-$MeOC_6H_4C{\equiv}CH$	**2a**	6.06(8)
2	*p*-$MeC_6H_4C{\equiv}CH$	**2b**	4.14(3)
3	PhC≡CH	**2c**	4.71(6)
4	*p*-$BrC_6H_4C{\equiv}CH$	**2d**	2.89(4)
5	*p*-$MeO_2CC_6H_4C{\equiv}CH$		very slow
6	*t*-BuC≡CH	**2e**	3.10(4)
7	FcC≡CH	**2f**	7.4(2)

[a] All reactions were run in $ClCH_2CH_2Cl$ at 50 °C. Initial concentration: $[\mathbf{1}]_0 = 15$ mM, $[alkyne]_0 = 150$ mM, $[MeCN]_0 = 40$ mM.

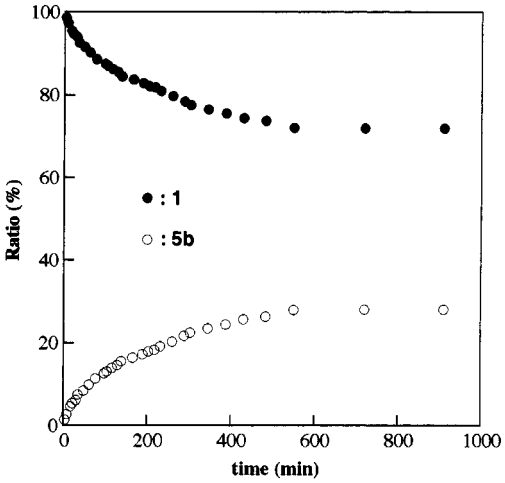

Figure 3. Time course of the reaction of **1** with $Me_3SiC{\equiv}CSiMe_3$ in $ClCH_2CH_2Cl$ at 50 °C. Initial concentration: $[\mathbf{1}]_0 = 15$ mM, $[Me_3SiC{\equiv}CSiMe_3]_0 = 0.15$ M.

Reactions of $RuCl_2$(NCMe)(dcpmp) (1) with Silylalkynes. Unlike the reactions of terminal alkynes, the reactions of **1** with silylalkynes afforded equilibrium mixtures of **1** and β-silylvinylidene complexes (eq 5). Figure 3 shows the time course of the reaction of **1** with

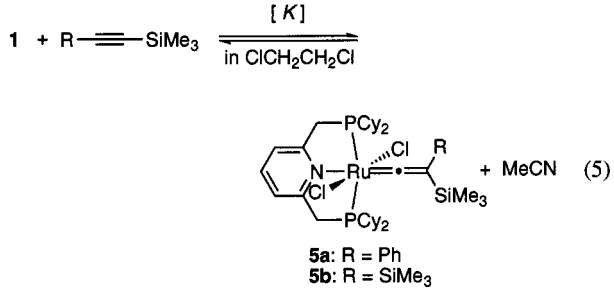

$Me_3SiC{\equiv}CSiMe_3$ in $ClCH_2CH_2Cl$ at 50 °C. The conversion of **1** into **5b** obeyed pseudo-first-order kinetics ($k_{obsd} = 0.24 \times 10^{-4}$ sec^{-1}) over 10 h to reach the equilibrium with $K(\mathbf{5b}/\mathbf{1}) = [\mathbf{5b}][MeCN]/[\mathbf{1}][Me_3SiC{\equiv}CSiMe_3] = 11.3 \times 10^{-3}$ ($\Delta G_{323} = 2.9$ kcal mol^{-1}). Almost the same equilibrium constant (12×10^{-3}) was observed for the reverse reaction system starting from **5b** and MeCN (1 equiv). A similar set of experiments was carried out for the interconversion between **1** and **5a**, and the following equilibrium constant was obtained: $K(\mathbf{5a}/\mathbf{1}) = [\mathbf{5a}][MeCN]/[\mathbf{1}][PhC{\equiv}CSiMe_3] = 3.9 \times 10^{-3}$ ($\Delta G_{323} = 3.5$

Table 3. Characteristic NMR Data for 2a−2f, 5a, and 5b[a]

	^{1}H NMR	^{13}C{^{1}H} NMR[b]		
complex	H$^\beta$	C$^\alpha$	C$^\beta$	^{31}P{^{1}H} NMR
2a	5.08 (s)	363.6 (t, 12)	112.1 (s)	46.7 (s)
2b	5.06 (s)	363.3 (t, 11)	112.3 (s)	46.4 (s)
2c	5.09 (s)	362.0 (t, 11)	112.5 (s)	46.1 (s)
2d	4.98 (s)	361.0 (t, 12)	111.3 (s)	45.7 (s)
2e	3.69 (s)	361.8 (t, 12)	118.2 (s)	43.6 (s)
2f	4.72 (s)	360.3 (t, 11)	107.7 (s)	48.5 (s)
5a		340.8 (t, 12)	110.3 (s)	44.0 (s)
5b		*c*	*c*	40.9 (s)

[a] In $CDCl_3$ at 20 °C. Chemical shifts are reported in δ (ppm). [b] Numbers in parentheses are $^2J_{PC}$ values in Hz. [c] ^{13}C{^{1}H} NMR analysis was not feasible due to low solubility of the complex.

Table 4. Selected Bond Distances (Å) and Angles (deg) and Dihedral Angles between Least-Squares Planes (deg) for 2c and 5a

	2c	**5a**
Ru−C(1)	1.816(6)	1.845(4)
Ru−Cl(1)	2.427(1)	2.4152(9)
Ru−Cl(2)	2.418(1)	2.4023(9)
Ru−N	2.218(4)	2.200(3)
Ru−P(1)	2.375(2)	2.3595(9)
Ru−P(2)	2.355(2)	2.3635(9)
C(1)−C(2)	1.310(8)	1.301(5)
Ru−C(1)−C(2)	172.3(5)	177.2(3)
Cl(1)−Ru−Cl(2)	173.22(5)	167.22(3)
P(1)−Ru−P(2)	160.28(5)	162.10(3)
N−Ru−C(1)	176.5(2)	179.4(1)
(Ru, Cl(1), Cl(2), C(1)) vs (C(1), C(2), C(3))	63.48(3)	4.99(9)

kcal mol^{-1}). Thus the slightly higher stability of **5b** than **5a** was suggested.

The reaction of **1** was tested also with FcC≡CSiMe$_3$, *p*-MeOC$_6$H$_4$C≡CSiMe$_3$, and *p*-MeO$_2$CC$_6$H$_4$C≡CSiMe$_3$. While the formation of the vinylidene complex was noted for all silylalkynes by NMR spectroscopy, partial desilylation giving nonsilylated vinylidene complexes simultaneously took place,[10a] and no reproducible data were therefore obtained.

The β-silylvinylidene complex **5a** was found to be much less stable than **2c** derived from phenylacetylene as a terminal alkyne. Thus the treatment of **5a** with phenylacetylene in ClCH$_2$CH$_2$Cl at 50 °C resulted in quantitative formation of **2c**, while the reverse reaction of **2c** with PhC≡CSiMe$_3$ did not take place.

Identification of Vinylidene Complexes. We have described the formation of **2a**−**2f**, **5a**, and **5b** from **1**. These complexes could be synthesized more conveniently starting from [RuCl$_2$(*p*-cymene)]$_2$ (eq 6). Reac-

$$\text{1/2 [RuCl}_2\text{(}p\text{-cymene)]}_2 + \text{dcpmp} + \text{R—}\equiv\text{—Z} \xrightarrow[-\,p\text{-cymene}]{\text{toluene, 80 °C}} \textbf{2a–2f, 5a,} \text{ and } \textbf{5b} \quad (6)$$

tions of the *p*-cymene complex with dcpmp and alkynes in toluene proceeded at 80 °C to afford the vinylidene complexes in 94−40% isolated yields.

Table 3 lists the selected NMR data. The ^{13}C{^{1}H} NMR spectra exhibited characteristic signals of α- and β-vinylidene carbons at δ 363.6−340.8 and 118.2−107.7, respectively. The α-carbon was observed as a triplet due to coupling with the two phosphorus nuclei of the dcpmp ligand ($^2J_{PC}$ = 11 or 12 Hz), whereas the β-carbon was a singlet. Complexes **2a**−**2f** exhibited a singlet signal at δ 5.09−3.69 assignable to the vinylidene proton. Although ^{13}C{^{1}H} NMR analysis of **5b** was not feasible owing to its low solubility, the presence of the vinylidene ligand was clearly indicated by the appearance of strong $\nu_{C=C}$ absorptions at 1605 and 1560 cm^{-1} in the IR spectrum.

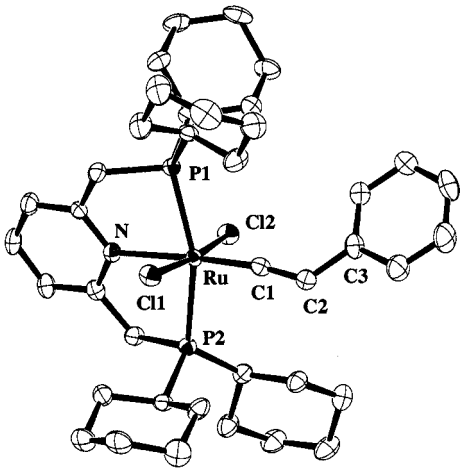

Figure 4. Molecular structure of RuCl$_2$(=C=C(H)Ph}-(dcpmp) (**2c**). Thermal ellipsoids are drawn at the 50% probability level. Solvent molecule is omitted for clarity.

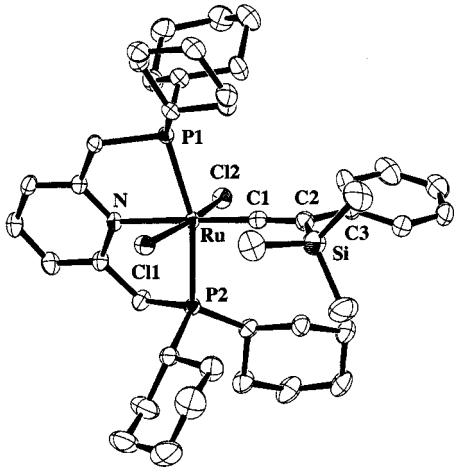

Figure 5. Molecular structure of RuCl$_2$(=C=C(SiMe$_3$)-Ph}(dcpmp) (**5a**). Thermal ellipsoids are drawn at the 50% probability level.

Complexes **2c** and **5a** were further examined by single-crystal X-ray diffraction analysis. Selected structural parameters are listed in Table 4. ORTEP diagrams are given in Figures 4 and 5. Both complexes adopt a distorted octahedral configuration with meridional coordination of the dcpmp ligand. The two chloro ligands are oriented in mutually trans positions, while the vinylidene ligand is situated trans to the pyridyl group of dcpmp.

The Ru−C(1) distances of **2c** (1.816(6) Å) and **5a** (1.845(4) Å) are in a typical range of six-coordinate vinylideneruthenium(II) complexes,[14] but significantly longer than that of five-coordinate complexes having a square pyramidal structure with the vinylidene ligand

(14) (a) Bruce, M. I. *Chem. Rev.* **1991**, *91*, 197−257. (b) Bruce, M. I.; Swincer, A. G. *Adv. Organomet. Chem.* **1983**, *22*, 59−128.

at the apical position: $RuBr_2(=C=CHPh)(PPh_3)_2$ (1.768(17) Å),[15] $RuCl_2(=C=CHPh)(PPr^i_3)_2$ (1.750(4) Å),[10a] $RuCl_2(=C=CHPh)(PCy_3)_2$ (1.761(2) Å),[10a] and $RuCl_2\{=C=C(SePr^i)Ph\}(PPh_3)_2$ (1.769(5) Å).[16] On the other hand, the C(1)−C(2) bond of the vinylidene ligand in **2c** (1.310(8) Å) and **5a** (1.301(5) Å) is apparently shorter than that of the five-coordinate complexes (1.33−1.36 Å). Thus the coordination of the pyridine donor in **2c** and **5a** elongates the Ru−C(1) bond to reduce the π-back-donation from ruthenium to the vinylidene ligand, leading to the shorter C(1)−C(2) bond than that in the five-coordinate analogues.

Discussion

We could measure the rates of formation of vinylidene complexes **2** from **1** and terminal alkynes (Table 2). While the reactivity is affected by both the electronic and steric nature of the R groups, the kinetic data observed for five kinds of phenylacetylene derivatives (p-$YC_6H_4C{\equiv}CH$) reveal that the more electron-donating substituent Y tends to give the higher reaction rate (runs 1−5). As described in Scheme 1 using phenylacetylene as a substrate, vinylidene complexes **2** are formed by the sequence of three elementary processes (i.e., dissociation of MeCN, coordination of alkyne, and tautomerization of alkyne ligand into vinylidene ligand). Of these elementary processes, the dissociation of MeCN is independent of alkynes, whereas the rates of the other processes must be dependent on the nature of the alkynes. Since the formation of alkyne complexes **4** is easier for more electron-deficient alkynes in a general sense, we may consider that the variation in the reaction rates of five phenylacetylene derivatives is mainly due to the rate difference in the final elementary process leading to the tautomerization of alkyne ligand into vinylidene ligand. This consideration is also supported by the kinetic findings for the reaction of phenylacetylene ($k_{-1}/k_2 = 20(2)$, $k_H/k_D = 1.69(5)$). Therefore, we may conclude that, at least for the phenylacetylene derivatives, the alkyne−vinylidene tautomerization is facilitated by increasing electron-donating ability of the R groups.

Experimental Section

General Procedure and Materials. All manipulations were performed under a nitrogen atmosphere using conventional Schlenk techniques. Nitrogen gas was purified by passing through a column of P_2O_5 (Merck, SICAPENT). NMR spectra were recorded on a Varian Mercury 300 (^{1}H NMR, 300.11 MHz; ^{13}C NMR, 75.46 MHz; ^{31}P NMR, 121.49 MHz) spectrometer. Chemical shifts are reported in δ (ppm), referenced to the ^{1}H (of residual protons) and ^{13}C signals of deuterated solvents or to the ^{31}P signal of external 85% H_3PO_4. The symbol J_{app} stands for the apparent coupling constant for a virtually coupled signal. IR spectra were recorded on a JASCO FT/IR-410 instrument. Mass spectra were measured with a Shimadzu QP-5000 GC-mass spectrometer (EI, 70 eV).

CH_2Cl_2, $ClCH_2CH_2Cl$, and MeCN were dried over CaH_2. Methanol was dried with $Mg(OMe)_2$. THF and toluene were dried over sodium benzophenone ketyl. These solvents were distilled under a nitrogen atmosphere and stored over molecular sieves (MS4A), which were activated by heating at ca. 300 °C under vacuum overnight prior to use. $CDCl_3$ was purified by passage through an alumina column, degassed by freeze−pump−thaw cycles, and stored over activated MS4A in the dark. Liquid alkynes were degassed by freeze−pump−thaw cycles prior to use. $[RuCl_2(p\text{-cymene})]_2$,[17] p-$MeOC_6H_4C{\equiv}CH$,[18] p-$BrC_6H_4C{\equiv}CH$,[19] and $FcC{\equiv}CH$[20] were synthesized according to the literatures. All other chemicals were obtained from commercial suppliers and used without further purification.

Synthesis of 2,6-Bis{(dicyclohexylphosphino)methyl}-pyridine (dcpmp). To a solution of dicyclohexylphosphine (2.65 g, 13.4 mmol) in THF (25 mL) was added dropwise a solution of *n*-butyllithium in hexane (1.6 M, 8.5 mL, 14 mmol) at −78 °C. The mixture was stirred at room temperature for 1 h to give a pale yellow solution of lithium dicyclohexylphosphide. This solution was added dropwise through a cannula to a solution of 2,6-bis(chloromethyl)pyridine (1.18 g, 6.70 mmol) in THF (20 mL) at 0 °C. The resulting orange solution was stirred at room temperature for 18 h. Methanol (6 mL) was slowly added, and then the mixture was concentrated by pumping to dryness. The yellowish white solid thus obtained was extracted with CH_2Cl_2 (5 mL × 2), and the extract was filtered through a short column of alumina. The combined filtrate was evaporated by pumping. The residue was washed with methanol (15 mL × 3) and dried under vacuum to give a white solid of dcpmp (1.76 g, 53%). Mp: 59−60 °C. ^{1}H NMR ($CDCl_3$): δ 7.42 (t, J = 7.5 Hz, 1H, H^4 of pyridine ring), 7.08 (d, J = 7.5 Hz, 2H, H^{3,5} of pyridine ring), 2.95 (d, $^2J_{PH}$ = 2.1 Hz, 4H, PCH_2), 1.90−1.56, 1.39−1.05 (each m, 44H, Cy). ^{13}C{^{1}H} NMR ($CDCl_3$): δ 159.9 (d, $^2J_{PC}$ = 10 Hz, C^{2,6} of pyridine ring), 135.9 (s, C^4 of pyridine ring), 120.2 (d, $^3J_{PC}$ = 9 Hz, C^{3,5} of pyridine ring), 33.4 (d, $^1J_{PC}$ = 14 Hz, PCH_2), 31.9 (d, $^1J_{PC}$ = 21 Hz, C^1 of Cy), 29.8 (d, $^2J_{PC}$ = 14 Hz, C^{2,6} of Cy), 29.0 (d, $^3J_{PC}$ = 9 Hz, C^{3,5} of Cy), 26.4 (s, C^4 of Cy). ^{31}P{^{1}H} NMR ($CDCl_3$): δ 3.8 (s). Anal. Calcd for $C_{31}H_{51}NP_2$: C, 74.51; H, 10.29; N, 2.80. Found: C, 74.31; H, 10.24; N, 3.04.

Synthesis of Acetonitrile Complex 1. To a suspension of $[RuCl_2(p\text{-cymene})]_2$ (370 mg, 0.604 mmol) in toluene (20 mL) were added dcpmp (605 mg, 1.21 mmol) and acetonitrile (0.64 mL, 12 mmol) at room temperature. The mixture was stirred at 80 °C for 22 h and then cooled to room temperature. The orange microcrystalline solid of **1** thus precipitated was collected by filtration through a filter-paper-tipped cannula, washed with pentane (5 mL × 3), and dried under vacuum (0.557 g, 65%). Mp: 280−283 °C (dec). ^{1}H NMR ($CDCl_3$): δ 7.23 (t, J = 7.5 Hz, H^4 of pyridine ring), 7.04 (d, J = 7.5 Hz, H^{3,5} of pyridine ring), 3.72 (virtual triplet, J_{app} = 4.2 Hz, 4H, PCH_2), 2.60−2.51, 2.00−1.66, 1.38−1.22 (each m, 44H, Cy), 2.35 (s, 3H, MeCN). ^{13}C{^{1}H} NMR ($CDCl_3$): δ 166.2 (virtual triplet, J_{app} = 5 Hz, C^{2,6} of pyridine ring), 134.1 (s, C^4 of pyridine ring), 125.7 (s, RuN*C*Me), 119.3 (virtual triplet, J_{app} = 5 Hz, C^{3,5} of pyridine ring), 37.8 (virtual triplet, J_{app} = 9 Hz, PCH_2), 34.8 (virtual triplet, J_{app} = 9 Hz, C^1 of Cy), 29.3, 28.8 (each s, C^{3,5} of Cy), 27.6, 27.2 (each virtual triplet, J_{app} = 6 Hz, C^{2,6} of Cy), 26.1 (s, C^4 of Cy), 4.7 (s, RuNC*Me*). ^{31}P{^{1}H} NMR ($CDCl_3$): δ 44.6 (s). IR (KBr): 2265 cm^{-1}. Anal. Calcd for $C_{33}H_{54}Cl_2N_2P_2Ru$: C, 55.61; H, 7.64; N, 3.93. Found: C, 55.40; H, 7.70; N, 4.07.

Reaction of 1 with Alkynes. A typical procedure (entry 1 in Table 1) is as follows. A 5 mm NMR sample tube equipped with a rubber septum cap was charged with **1** (7.6 mg, 11 μmol), and the system was replaced with nitrogen gas. 1,2-Dichloroethane (0.7 mL) was added by syringe, and the

(15) Wakatsuki, Y.; Koga, N.; Yamazaki, H.; Morokuma, K. *J. Am. Chem. Soc.* **1994**, *116*, 8105−8111.
(16) Hill, A. F.; Hulkes, A. G.; White, A. J. P.; Williams, D. J. *Organometallics* **2000**, *19*, 371−373.
(17) Bennett, M. A.; Smith, A. K. *J. Chem. Soc., Dalton Trans.* **1974**, 233−241.
(18) Takahashi, S.; Kuroyama, Y.; Sonogashira, K.; Hagihara, N. *Synthesis* **1980**, 627−630.
(19) Jacobs, T. L. *Org. React.* **1949**, *5*, 50−51.
(20) Doisneau, G.; Balavoine, G.; Fillebeen-Khan, T. *J. Organomet. Chem.* **1992**, *425*, 113−117.

mixture was gently shaken until all the complex dissolved. To the resulting yellow solution were succesively added MeCN (1.1 mg, 27 μmol) and PhC≡CH (10.7 mg, 0.105 mmol) at room temperature. The sample was immediately inserted into an NMR probe preheated at 50 ± 0.1 °C and kept at this temperature throughout the experiment. The time course of the reaction was followed by measuring relative peak integration of **1** (δ 44.5) and **2c** (δ 46.0) in the $^{31}P\{^1H\}$ NMR spectra.

Synthesis of Vinylidene Complexes 2a−2f, 5a, and 5b. A typical procedure is as follows. A mixture of $[RuCl_2(p\text{-cymene})]_2$ (204 mg, 0.333 mmol), dcpmp (334 mg, 0.668 mmol), and PhC≡CH (68 mg, 0.67 mmol) in toluene (11 mL) was heated at 80 °C for 32 h with vigorous stirring. An initially red suspension was gradually changed into a dark red solution, which was allowed to stand at room temperature and then at −20 °C overnight to yield a reddish brown precipitate of **2c**, which was collected by filtration, washed with toluene (2 mL), and dried under vacuum (483 mg, 94%). This product was spectroscopucally pure. An analytically pure crystalline compound was obtained by slow diffusion of a CH_2Cl_2 solution into hexane. The other vinylidene complexes were similarly prepared. For **2e** an excess amount (10 equiv/Ru) of *tert*-butylacetylene was nescessary.

$RuCl_2${=C=C(H)C_6H_4OMe-*p*}(dcpmp) (2a): gray solid (40%); mp 230−232 °C (dec); ^1H NMR ($CDCl_3$) δ 7.63 (t, J = 7.7 Hz, 1H, H^4 of pyridine ring), 7.30 (d, J = 7.7 Hz, 2H, $H^{3,5}$ of pyridine ring), 7.13, 6.77 (each d, J = 8.2 Hz, 4H, C_6H_4), 5.08 (s, 1H, =C=CH), 3.91 (virtual triplet, J_{app} = 4.1 Hz, 4H, PCH_2), 3.77 (s, 3H, OMe), 2.61−2.42, 2.14−1.42, 1.32−1.13 (each m, 44H, Cy); $^{13}C\{^1H\}$ NMR ($CDCl_3$) δ 363.6 (t, $^2J_{PC}$ = 12 Hz, Ru=*C*=C), 161.3 (virtual triplet, J_{app} = 4 Hz, $C^{2,6}$ of pyridine ring), 156.6 (s, C^4 of C_6H_4OMe), 138.4 (s, C^4 of pyridine ring), 127.3, 113.7 (each s, $C^{2,3,5,6}$ of C_6H_4OMe), 124.0 (s, C^1 of C_6H_4OMe), 120.9 (virtual triplet, J_{app} = 4 Hz, $C^{3,5}$ of pyridine ring), 112.1 (s, Ru=C=*C*), 55.3 (s, OMe), 38.2 (virtual triplet, J_{app} = 11 Hz, C^1 of Cy), 34.5 (virtual triplet, J_{app} = 10 Hz, PCH_2), 29.4, 28.8 (each s, $C^{3,5}$ of Cy), 27.5, 27.2 (each virtual triplet, J_{app} = 6 Hz, $C^{2,6}$ of Cy), 26.0 (s, C^4 of Cy); $^{31}P\{^1H\}$ NMR ($CDCl_3$) δ 46.7 (s); IR (KBr) 1623, 1599 cm^{-1}. Anal. Calcd for $C_{40}H_{59}Cl_2NOP_2Ru$: C, 59.77; H, 7.40; N, 1.74. Found: C, 60.52; H, 7.88; N, 1.71.

$RuCl_2${=C=C(H)C_6H_4Me-*p*}(dcpmp) (2b): dark green solid (90%); mp 245−250 °C (dec); ^1H NMR ($CDCl_3$) δ 7.63 (t, J = 7.7 Hz, 1H, H^4 of pyridine ring), 7.30 (d, J = 7.7 Hz, 2H, $H^{3,5}$ of pyridine ring), 7.09, 6.99 (each d, J = 8.1 Hz, 4H, C_6H_4), 5.06 (s, 1H, =C=CH), 3.90 (virtual triplet, J_{app} = 4.2 Hz, 4H, PCH_2), 2.32 (s, 3H, Me), 2.55−2.47, 2.17−1.44, 1.30−1.14 (each m, 44H, Cy); $^{13}C\{^1H\}$ NMR ($CDCl_3$) δ 363.3 (t, $^2J_{PC}$ = 11 Hz, Ru=*C*=C), 161.3 (virtual triplet, J_{app} = 4 Hz, $C^{2,6}$ of pyridine ring), 138.4 (s, C^4 of pyridine ring), 133.2 (s, C^1 of C_6H_4), 129.0, 128.7, 126.1 (each s, C^{2-6} of C_6H_4), 120.9 (virtual triplet, J_{app} = 4 Hz, $C^{3,5}$ of pyridine ring), 112.3 (s, Ru=C=*C*), 38.2 (virtual triplet, J_{app} = 11 Hz, C^1 of Cy), 34.5 (virtual triplet, J_{app} = 10 Hz, PCH_2), 29.4, 28.8 (each s, $C^{3,5}$ of Cy), 27.5, 27.2 (each virtual triplet, J_{app} = 6 Hz, $C^{2,6}$ of Cy), 26.0 (s, C^4 of Cy), 21.1 (s, Me); $^{31}P\{^1H\}$ NMR ($CDCl_3$) δ 46.4 (s); IR (KBr) 1623, 1603 cm^{-1}. Anal. Calcd for $C_{40}H_{59}Cl_2NP_2Ru$: C, 60.98; H, 7.55; N, 1.78. Found: C, 61.18; H, 7.78; N, 1.75.

$RuCl_2${=C=C(H)Ph}(dcpmp) (2c): mp 192−195 °C (dec); ^1H NMR ($CDCl_3$) δ 7.63 (t, J = 8.0 Hz, 1H, H^4 of pyridine ring), 7.30 (d, J = 8.0 Hz, 2H, $H^{3,5}$ of pyridine ring), 7.21−7.15, 6.94−6.90 (m, 5H, Ph), 5.09 (s, 1H, =C=CH), 3.91 (virtual triplet, J_{app} = 4.0 Hz, 4H, PCH_2), 2.55−2.47, 2.16−1.45, 1.30−1.14 (each m, 44H, Cy); $^{13}C\{^1H\}$ NMR ($CDCl_3$) δ 362.0 (t, $^2J_{PC}$ = 11 Hz, Ru=*C*=C), 161.3 (virtual triplet, J_{app} = 4 Hz, $C^{2,6}$ of pyridine ring), 138.5 (s, C^4 of pyridine ring), 132.6 (s, C^1 of Ph), 128.0, 126.1, 123.8 (each s, C^{2-6} of Ph), 120.9 (virtual triplet, J_{app} = 4 Hz, $C^{3,5}$ of pyridine ring), 112.5 (s, Ru=C=*C*), 38.1 (virtual triplet, J_{app} = 11 Hz, C^1 of Cy), 34.5 (virtual triplet, J_{app} = 10 Hz, PCH_2), 29.4, 28.9 (each s, $C^{3,5}$ of Cy), 27.5, 27.2 (each virtual triplet, J_{app} = 6 Hz, $C^{2,6}$ of Cy), 26.0 (s, C^4 of Cy); $^{31}P\{^1H\}$ NMR ($CDCl_3$) δ 46.1 (s); IR (KBr) 1617, 1591 cm^{-1}. Anal. Calcd for $C_{39}H_{57}Cl_2NP_2Ru$: C, 60.54; H, 7.42; N, 1.81. Found: C, 60.80; H, 7.50; N, 1.79.

$RuCl_2${=C=C(H)C_6H_4Br-*p*}(dcpmp) (2d): brown solid (95%); mp 125−128 °C (dec); ^1H NMR ($CDCl_3$) δ 7.65 (t, J = 7.5 Hz, 1H, H^4 of pyridine ring), 7.31 (d, J = 7.5 Hz, 2H, $H^{3,5}$ of pyridine ring), 7.26, 7.06 (each d, J = 8.4 Hz, 4H, C_6H_4), 4.98 (s, 1H, =C=CH), 3.91 (virtual triplet, J_{app} = 4.2 Hz, 4H, PCH_2), 2.59−2.44, 2.16−1.42, 1.33−1.12 (each m, 44H, Cy); $^{13}C\{^1H\}$ NMR ($CDCl_3$) δ 361.0 (t, $^2J_{PC}$ = 12 Hz, Ru=*C*=C), 161.3 (virtual triplet, J_{app} = 4 Hz, $C^{2,6}$ of pyridine ring), 138.6 (s, C^4 of pyridine ring), 131.9, 130.9, 127.3 (each s, C^{2-6} of C_6H_4-Br), 121.0 (virtual triplet, J_{app} = 4 Hz, $C^{3,5}$ of pyridine ring), 116.4 (s, C^1 of C_6H_4Br), 111.3 (s, Ru=C=*C*), 38.1 (virtual triplet, J_{app} = 11 Hz, C^1 of Cy), 34.5 (virtual triplet, J_{app} = 10 Hz, PCH_2), 29.5, 28.9 (each s, $C^{3,5}$ of Cy), 27.5, 27.2 (each virtual triplet, J_{app} = 6 Hz, $C^{2,6}$ of Cy), 26.0 (s, C^4 of Cy); $^{31}P\{^1H\}$ NMR ($CDCl_3$) δ 45.7 (s); IR (KBr) 1625, 1600 cm^{-1}. Anal. Calcd for $C_{39}H_{56}BrCl_2NP_2Ru$: C, 54.93; H, 6.62; N, 1.64. Found: C, 55.66; H, 6.05; N, 1.59.

$RuCl_2${=C=C(H)Bu^t}(dcpmp) (2e): reddish brown solid (76%); mp 95−97 °C; ^1H NMR ($CDCl_3$) δ 7.58 (t, J = 7.7 Hz, 1H, H^4 of pyridine ring), 7.27 (d, J = 7.7 Hz, 2H, $H^{3,5}$ of pyridine ring), 5.30 (s, 2H, CH_2Cl_2), 3.90 (virtual triplet, J_{app} = 4.2 Hz, 4H, PCH_2), 3.69 (s, 1H, Ru=C=CH), 2.60−2.48, 2.31−2.20, 2.06−1.95, 1.90−1.46, 1.36−1.13 (each m, 44H, Cy), 1.20 (s, *t*-Bu); $^{13}C\{^1H\}$ NMR ($CDCl_3$) δ 361.8 (t, $^2J_{PC}$ = 12 Hz, Ru=*C*=C), 161.9 (virtual triplet, J_{app} = 4 Hz, $C^{2,6}$ of pyridine ring), 138.2 (s, C^4 of pyridine ring), 120.6 (virtual triplet, J_{app} = 4 Hz, $C^{3,5}$ of pyridine ring), 118.2 (t, $^3J_{PC}$ = 2 Hz, Ru=C=*C*), 54.2 (s, CH_2Cl_2), 38.6 (virtual triplet, J_{app} = 10 Hz, C^1 of Cy), 34.8 (virtual triplet, J_{app} = 10 Hz, PCH_2), 32.6 (s, $C(CH_3)_3$), 31.2 (s, $C(CH_3)_3$), 29.7, 29.0 (each s, $C^{3,5}$ of Cy), 27.5, 27.2 (each virtual triplet, J_{app} = 6 Hz, $C^{2,6}$ of Cy), 26.1 (s, C^4 of Cy); $^{31}P\{^1H\}$ NMR ($CDCl_3$) δ 43.6 (s); IR (KBr) 1602, 1571 cm^{-1}. Anal. Calcd for $C_{37}H_{61}Cl_2NP_2Ru\cdot CH_2Cl_2$: C, 54.42; H, 7.57; N, 1.67. Found: C, 54.21; H, 6.98; N, 1.21.

$RuCl_2${=C=C(H)Fc}(dcpmp) (2f): dark brown solid (58%); mp 263−265 °C (dec); ^1H NMR ($CDCl_3$) δ 7.60 (t, J = 7.5 Hz, 1H, H^4 of pyridine ring), 7.28 (d, J = 7.5 Hz, 2H, $H^{3,5}$ of pyridine ring), 4.72 (s, 1H, Ru=C=C*H*), 4.16, 4.03 (each s, 4H, C_5H_4Fe), 4.12 (s, 5H, C_5H_5Fe), 3.88 (virtual triplet, J_{app} = 4.2 Hz, 4H, PCH_2), 3.69 (s, 1H, Ru=C=CH), 2.60−2.42, 2.20−2.08, 1.98−1.40, 1.36−1.13 (each m, 44H, Cy); $^{13}C\{^1H\}$ NMR ($CDCl_3$) δ 360.3 (t, $^2J_{PC}$ = 11 Hz, Ru=*C*=C), 161.3 (virtual triplet, J_{app} = 4 Hz, $C^{2,6}$ of pyridine ring), 138.2 (s, C^4 of pyridine ring), 120.8 (t, $^3J_{PC}$ = 4 Hz, $C^{3,5}$ of pyridine ring), 107.7 (s, Ru=C=*C*), 78.7 (s, C^1 of C_5H_4Fe), 69.0 (s, C_5H_5Fe), 66.9, 66.5 (each s, $C^{2,3,4,5}$ of C_5H_4Fe), 38.3 (virtual triplet, J_{app} = 10 Hz, C^1 of Cy), 34.5 (virtual triplet, J_{app} = 10 Hz, PCH_2), 29.4, 28.9 (each s, $C^{3,5}$ of Cy), 27.5, 27.1 (each virtual triplet, J_{app} = 6 Hz, $C^{2,6}$ of Cy), 26.0 (s, C^4 of Cy); $^{31}P\{^1H\}$ NMR ($CDCl_3$) δ 48.5 (s); IR (KBr) 1630, 1599 cm^{-1}. Anal. Calcd for $C_{43}H_{61}Cl_2NP_2FeRu$: C, 58.57; H, 6.97; N, 1.59. Found: C, 57.99; H, 6.82; N, 1.58.

$RuCl_2${=C=C(SiMe$_3$)Ph}(dcpmp) (5a): reddish brown solid (59%); mp 184−189 °C (dec); ^1H NMR ($CDCl_3$) δ 7.57 (t, J = 7.5 Hz, 1H, H^4 of pyridine ring), 7.32−7.18 (m, 6H, $H^{3,5}$ of pyridine ring and $H^{2,3,5,6}$ of Ph), 7.00 (t, J = 7.2 Hz, H^4 of Ph), 3.89 (virtual triplet, J_{app} = 4.0 Hz, 4H, PCH_2), 2.56−2.48, 2.26−2.08, 2.04−1.11 (each m, 44H, Cy), 0.27 (s, 9H, $SiMe_3$); $^{13}C\{^1H\}$ NMR ($CDCl_3$) δ 340.8 (t, $^2J_{PC}$ = 12 Hz, Ru=*C*=C), 161.8 (virtual triplet, J_{app} = 4 Hz, $C^{2,6}$ of pyridine ring), 138.0 (s, C^4 of pyridine ring), 132.1 (s, C^1 of Ph), 130.2, 127.3, 125.9 (each s, C^{2-6} of Ph), 120.5 (br, $C^{3,5}$ of pyridine ring), 110.3 (s, Ru=C=*C*), 38.2 (virtual triplet, J_{app} = 10 Hz, C^1 of Cy), 34.3 (virtual triplet, J_{app} = 10 Hz, PCH_2), 29.4, 28.8 (each s, $C^{3,5}$ of Cy), 27.3, 27.0 (each virtual triplet, J_{app} = 6 Hz, $C^{2,6}$ of Cy), 25.8 (s, C^4 of Cy), 1.0 (s, $SiMe_3$); $^{31}P\{^1H\}$ NMR ($CDCl_3$) δ 44.0 (s); IR (KBr) 1600, 1555 cm^{-1}. Anal. Calcd for $C_{42}H_{65}Cl_2NP_2RuSi$: C, 59.63; H, 7.74; N, 1.66. Found: C, 59.40; H, 7.85; N, 1.69.

Table 5. Crystallographic Data and Details of Structure Refinement for 2c and 5a

	2c	5a
formula	$C_{39}H_{57}Cl_2NP_2Ru{\cdot}CH_2Cl_2$	$C_{42}H_{65}Cl_2NP_2RuSi$
fw	858.74	845.99
cryst size (mm)	0.4 × 0.3 × 0.3	0.2 × 0.2 × 0.2
cryst syst	triclinic	monoclinic
space group	$P\bar{1}$ (No. 2)	$P2_1/c$ (No. 14)
a (Å)	12.708(2)	12.303(1)
b (Å)	14.262(1)	19.167(1)
c (Å)	12.386(1)	17.950(1)
α (deg)	96.413(9)	
β (deg)	112.023(8)	90.343(7)
γ (deg)	95.48(1)	
V (Å^3)	2045.0(4)	4232.9(6)
Z	2	4
μ(Mo Kα) (cm^{-1})	7.52	6.30
F(000)	896	1784
$2\theta_{max}$ (deg)	55.0	55.0
T (K)	198	198
transmn factor	0.92−1.00	0.94−1.00
scan width (deg)	1.37 + 0.35 tan θ	1.31 + 0.35 tan θ
scan type	$\omega-2\theta$	$\omega-2\theta$
scan rate (deg min^{-1})	16	16
no. reflns measd	9760	10151
no. unique reflns	9385 (R_{int} = 0.033)	9710 (R_{int} = 0.022)
no. observations	5888 ($I \geq 3\sigma(I)$)	6442 ($I \geq 3\sigma(I)$)
no. variables	463	443
R^a	0.079	0.054
$R_w{}^b$	0.125	0.091
GOF^c	1.18	1.18
max Δ/σ in final cycle	0.006	0.000
max. and min. peak (e Å^{-3})	1.18, −0.90	0.52, −0.35

^{a} $R = \sum(F_o^2 - F_c^2)/\sum F_o 2$. ^{b} $R_w = [\sum w(F_o^2 - F_c^2)^2/\sum w(F_o^2)^2]^{1/2}$, $w = 1/[\sigma^2(F_o^2)]$. ^{c} GOF = $[\sum w(|F_o| - |F_c|)^2/(N_o - N_p)]^{1/2}$, where N_o is the number of observations and N_v the number of variables.

$RuCl_2${=C=C(SiMe$_3$)$_2$}(dcpmp) (5b): reddish brown solid (65%); mp 215−219 °C (dec); ^{1}H NMR ($CDCl_3$) δ 7.52 (t, J = 7.8 Hz, 1H, H^4 of pyridine ring), 7.21 (d, J = 7.8 Hz, 1H, H^{3,5} of pyridine ring), 3.82 (virtual triplet, J_{app} = 3.9 Hz, 4H, 2 PCH_2), 2.66−2.44, 2.01−1.57, 1.29−1.11 (each m, 44H, 2 PCy_2), 0.25 (s, 18H, $SiMe_3$); ^{13}C{^{1}H} NMR analysis of this complex was not feasible due to its low solubility; ^{31}P{^{1}H} NMR ($CDCl_3$) δ 40.9 (s); IR (KBr) 1605, 1560 cm^{-1}. Anal. Calcd for $C_{39}H_{69}Cl_2NP_2RuSi_2$: C, 55.63; H, 8.26; N, 1.66. Found: C, 56.33; H, 8.18; N, 1.69.

Crystal Structure Determination of 2c and 5a. A summary of crystal data, intensity collection, and refinement parameters is reported in Table 5. Single crystals of **2c** and **5a**, which were grown by slow diffusion of saturated CH_2Cl_2 solutions into pentane at room temperature, were mounted on glass fibers with an epoxy resin adhesive. All measurements were performed at 198 K on a Rigaku AFC5R (for **2c**) or AFC7R (for **5a**) four-circle diffractometer using graphite-monochromated Mo Kα radiation (λ = 0.71069 Å). Unit cell dimensions were obtained from a least-squares treatment of the setting angles of 25 automatically centered reflections with 29° < 2θ < 30° (for **2c**) or 25° < 2θ < 29° (for **5a**). Diffraction data were collected up to the maximum 2θ value of 55.0° using the $\omega-2\theta$ scan technique and subsequently corrected for Lorentz and polarization effects. The data were also corrected for absorption based on azimuthal scans of three standard reflections. No significant decay in the standard reflections was noted throughout the measurements.

All calculations were performed with the Texsan Crystal Sturucture Analysis Package provided by Rigaku Corp. The scattering factors were taken from ref 21. The structures were solved by heavy atom Patterson methods (PATTY)[22] and expanded using Fourier techniques (DIRDIF94).[23] Each structure was refined by full-matrix least-squares with anisotropic thermal parameters for all non-hydrogen atoms. In the crystal structure of **2c**, the solvent molecules (CH_2Cl_2) were observed to be statically disordered. They were modeled with three different CH_2Cl_2 moieties and refined with complementary occupancy factors. In the final cycles of refinement, hydrogen atoms were located at idealized positions (d(C−H) = 0.95 Å) with isotropic temperature factors ($B_{iso} = 1.20B_{bonded\ atom}$) and were included in calculation without refinement of their parameters. The function minimized in least-squares was $\sum w(F_o^2 - F_c^2)^2$ ($w = 1/[\sigma^2(F_o^2)]$).

Supporting Information Available: Details of the structure determination of **2c** and **5a**, including a figure giving the atomic numbering scheme and tables of atomic coordinates, thermal parameters, and full bond distances and angles. This material is available free of charge via the Internet at http://pubs.acs.org.

OM020238R

(21) Cromer, D. T.; Waber, J. T. *International Tables for X-ray Crystallography*; The Kynoch Press: Birmingham, UK, 1974; Vol. IV.

(22) Beurskens, P. T.; Admiraal, G.; Beurskens, G.; Bosman, W. P.; Garcia-Granda, S.; Gould, R. O.; Smits, J. M. M.; Smykalla, C. *The PATTY and DIRDIF Program System*; Technical Report of the Crystallographic Laboratory; University of Nijmegen: Nijmegen, The Netherlands, 1992.

(23) Beurskens, P. T.; Admiraal, G.; Beurskens, G.; Bosman, W. P.; de Gelder, R.; Israel, R.; Smits, J. M. M. *The DIRDIF-94 Program System*; Technical Report of the Crystallographic Laboratory; University of Nijmegen: Nijmegen, The Netherlands, 1994.